



The Role of Urinary Modulators and Bacteria in the Development of Infectious Kidney Stones

Dr. Brendan Wallace, MD, MSc in surgery candidate

Supervisors: Dr. Hassan Razvi, Dr. Jeremy Burton, Dr. Jennifer Bjazevic
Lawson Health Research Institute, Burton Laboratory
London ON Canada

There is a significant amount of knowledge about the pathogenesis of kidney stones that is not well understood, and this is especially true for infectious kidney stones. Infectious kidney stones can be divided into calcium phosphate and struvite stone compositions and are thought to be formed because of urinary infection with a pathogenic organism. Historically, it was believed that urease producing bacteria lead to infectious stones by converting urea into ammonium and creating an alkaline urinary pH; however, the formation of these stones is not completely explained through this mechanism. This stone type has an important impact on patient outcomes as it has been shown to have a higher recurrence rate, lead to recurrent infections/sepsis, affect more vulnerable patients and have a high rate of surgical intervention. In the Burton Lab at Lawson Health Research Institute, we aimed to explore possible urinary

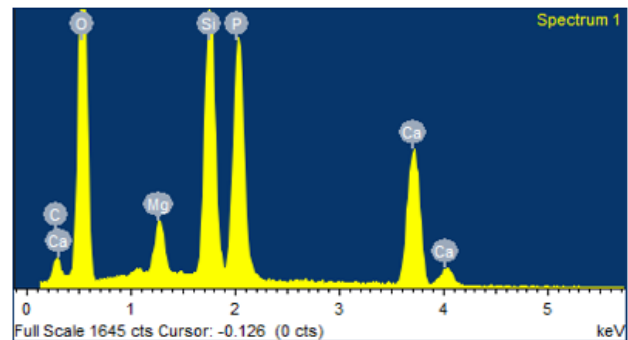
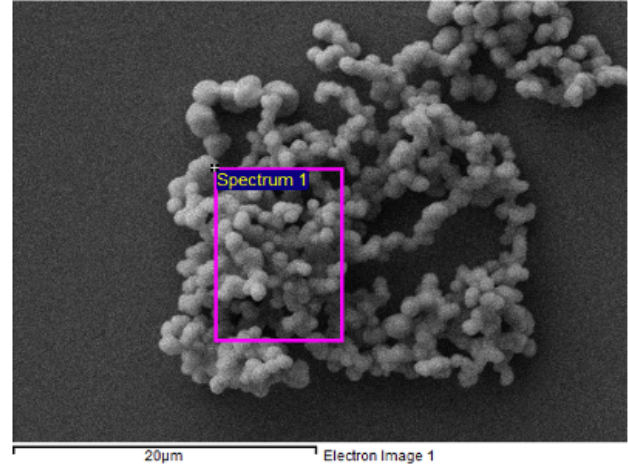
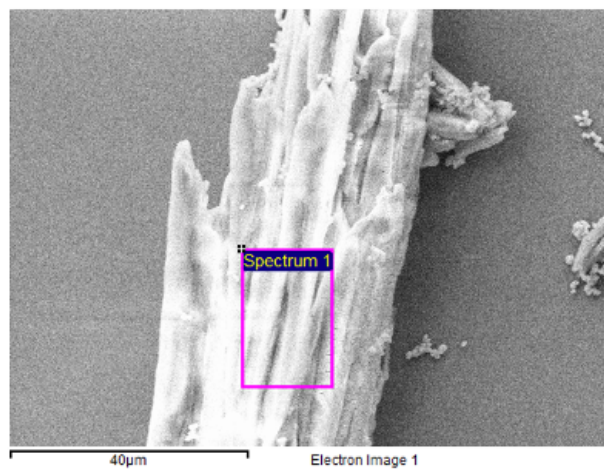


Figure 1: SEM/EDX of calcium phosphate

modulators in infectious stone development and to improve our understanding of the role of bacteria in the development of kidney stones. We developed a high-throughput experimental model, which uses Griffith's artificial urine and Jack Bean urease, to produce stone crystals within 24 hours. With the help of the Western Nanofabrication Facility, we validated this model by demonstrating the formation of both calcium phosphate (Figure 1) and struvite crystals (Figure 2).

Our model was then used to further examine the relationship between bacteria and stone formation. We examined the 10 most common bacterial species associated with struvite stone by isolating their intracellular proteins and incubating them in Griffith's artificial urine within our experimental model. After 24 hours of observation, we were able to observe various types of crystals form in



Electron Image 1

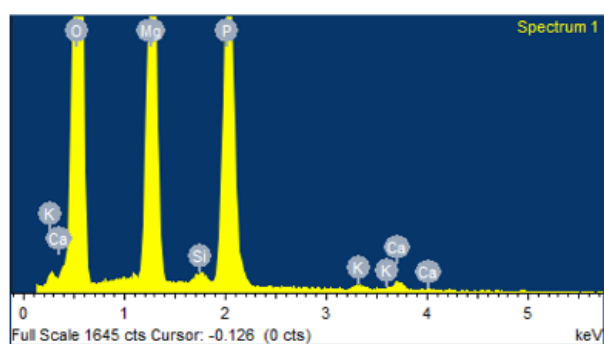


Figure 2: SEM/EDX of struvite crystals.

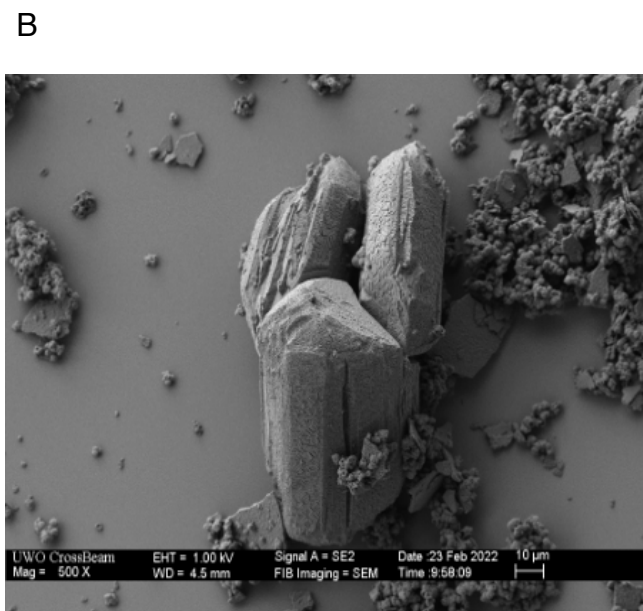
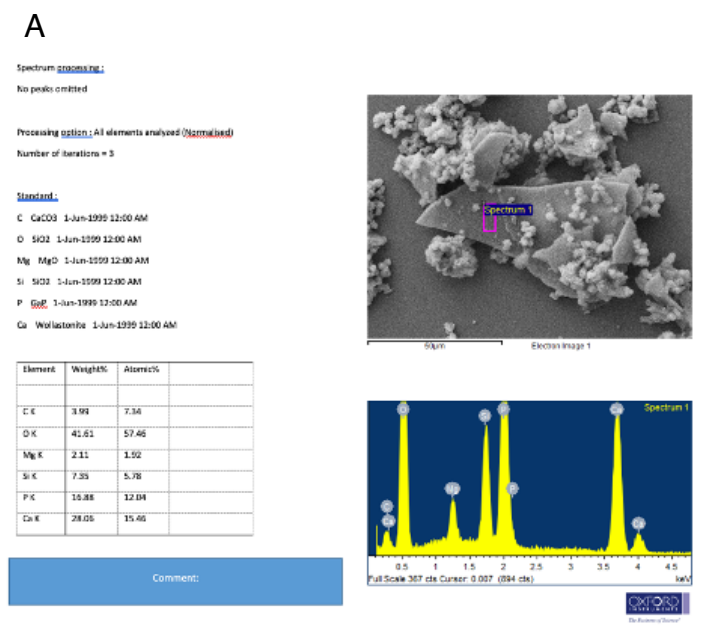


Figure 3: SEM/EDX analysis (A) and SEM photo of struvite and calcium phosphate crystals (B) from *Proteus mirabilis* 175A cell-free extract treatment.

Proteus mirabilis, *Klebsiella pneumoniae*, *Klebsiella oxytoca* and *Pseudomonas aeruginosa*. *Proteus mirabilis* 175A, originally isolated from a struvite kidney stone, produced both struvite and calcium phosphate crystals (Figure 3).

Interestingly, *Klebsiella oxytoca* produced a predominantly calcium oxalate stone (Figure 4) a composition that was not created in any other experimental condition that we performed. This is not a traditional infection-based stone, but it is the most common stone composition present in humans representing about 70-75% of kidney stones.

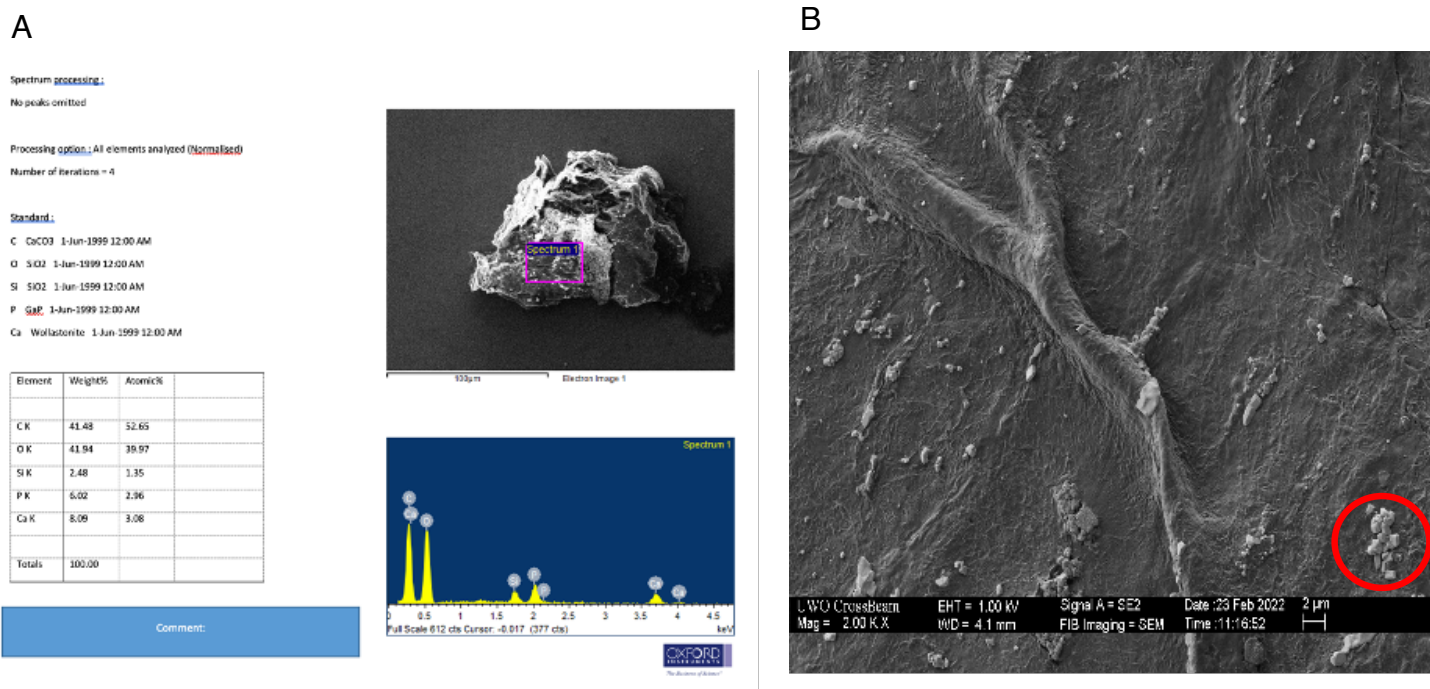


Figure 4: SEM/EDX analysis (A) and calcium oxalate crystals (B) from *Klebsiella oxytoca* RCA+2 cell-free extract treatment.

This novel discovery of calcium oxalate stones with *Klebsiella oxytoca* is very exciting. This suggests the possibility of an alternative mechanism for kidney stone formation with bacteria besides urease. This has important clinical implications because most urinary tract infections are not from urease producing bacteria. We plan to expand on this knowledge by sequencing the bacterial strains to potentially identify alternative metabolic pathways involved in kidney stone formation.

Acknowledgements: John Chmiel, Dr. Kait Al, Dr. Harvey Goldberg



Using Raman Spectroscopy to Determine Chemical Environment of Silver Nanoparticles in Plant Roots

Paul Boersma, Supervisor Dr. Sheila M Macfie

Department of Biology
Western University, London ON Canada

Due to their antimicrobial properties, silver nanoparticles are commonly found in personal cleaning products, industrial cleansers, baby clothes and toys, and sports clothing¹. They are also used in targeted drug delivery for ailments such as cancer, and to treat fungal and bacterial diseases of people² and crop plants³. Unfortunately, nanoparticles are inadvertently released down the drain and into the environment during material production, use, laundering and disposal⁴. During wastewater treatment, silver nanoparticles accumulate in biosolids⁵ (treated sewage sludge), which are commonly applied as a fertilizer on agricultural fields. Another source of silver nanoparticles to crop plants arises from their release into the air during waste incineration and subsequent settling on soil surfaces⁶.

My primary research goal was to determine the potential toxicity of silver nanoparticles to soybean and its symbiotic nitrogen-fixing bacterial partner. A secondary goal was to use Raman spectroscopy to determine the locations within soybean roots where silver nanoparticles accumulate. The Raman work was funded by a CAMBR Seed Grant (co-PIs, Sheila M Macfie and François Lagugné-Labarthet). Raman spectroscopy uses single wavelength lasers to excite molecular bonds, and different bond types have characteristic spectra. Silver (and other metals) amplify the signals arising from the bonds in surrounding molecules. For example, if silver accumulated in the cell walls within roots, the Raman signals for cellulose and lignin should be

stronger in roots of treated plants compared to those of control plants.

I discovered that as much as 2.5 µg/L of silver nanoparticles in hydroponic nutrient solution had no effect on soybean that were given adequate nitrogen; however, this treatment reduced biomass by 50% for plants that relied on symbiotic bacteria to obtain nitrogen. I determined that this was because the nitrogen-fixing bacteria were sensitive to the nanoparticles, and the development and activity of nitrogen-fixing nodules on the plant roots were hindered by as little as 0.5 to 2.5 µg/L of silver nanoparticles.

Using Raman spectroscopy to determine the location of silver within plant roots will require more method development. I was able to detect signals for cellulose, a major component of plant cell walls, as well as lignin, which is found in the walls of certain cell types. For example, the cell wall of a xylem vessel was associated with Raman signals for cellulose and lignin (Figure 1). However, the spectra for roots treated with silver nanoparticles were indistinguishable from control spectra (data not shown). The quality of the spectra was negatively affected by a few factors: fluorescence interference from the plant samples (especially leaves and stems); errant signals from the glass on which the samples were mounted (due to the laser passing through open spaces in the sample, such as xylem cells); and the concentrations of silver in the treated plants may have been too low to have a measurable effect on the Raman spectra.

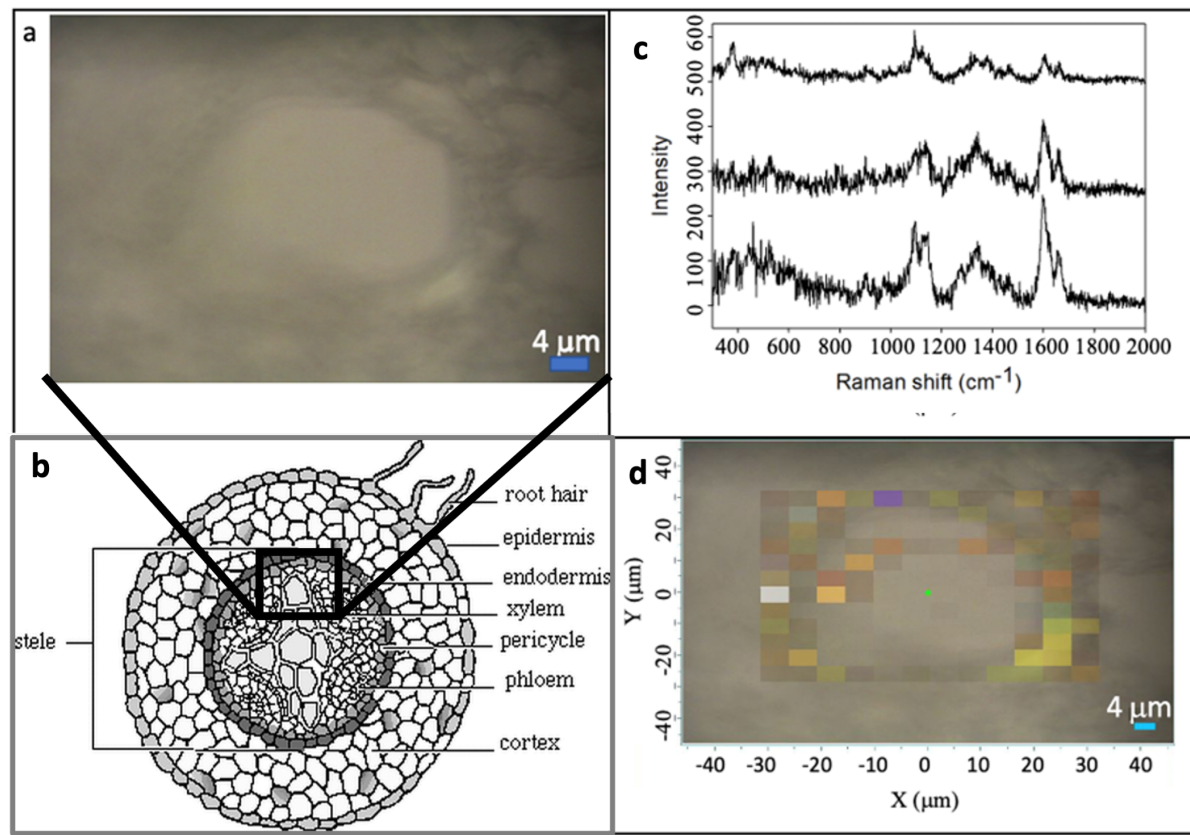


Figure 1: Raman spectroscopy of a xylem cell in a control soybean root. **Panel (a)** light microscope video image of area assessed; the large white area is a xylem cell. **Panel (b)** schematic representation of a typical root (from <http://plant-structure.weebly.com/blog/a-view-inside-a-dicot-root>), showing the approximate location of the region shown in panel a. **Panel (c)** Three representative spectra attained from Raman spectroscopy of control plants. The intensity is shifted for the two highest spectra for easier viewing. The Raman peak between 1045 and 1165 cm^{-1} represents cellulose, glucomannan and/or xylan; the peak between 1238 – 1522 cm^{-1} represents cellulose; the peak between 1549 – 1702 cm^{-1} represents lignin. **Panel (d)** video image of the control root in panel a) with overlapped maps for the three peaks of interest. The strongest spectrum was for lignin, which is expected in the wall of a xylem cell.

1. Vance et al. (2014) Nanotechnology in the real world: Redeveloping the nanomaterial consumer products inventory. *Beilstein J. Nanotechnol.* 6, 1769–1780. <https://doi.org/10.3762/bjnano.6.181>
2. Lombardo et al. (2019) Smart nanoparticles for drug delivery application: Development of versatile nanocarrier platforms in biotechnology and nanomedicine. *J. Nanomater.* 2019. <https://doi.org/10.1155/2019/3702518>
3. Hae-Jun (2006) A new composition of nanosized silica-silver for control of various plant diseases. *Plant Pathol. J.* 22(3): 295-302. <https://doi.org/10.5423/PPJ.2006.22.3.295>
4. Finnish Institute of Occupational Health (2017) NANOSOLUTIONS Final Report: Final publishable summary report 30. editors K. Savolainen and A. Vartio, <http://nanosolutionsfp7.com/final-report-and-publishable-summary/>
5. Schlich et al. (2013) Hazard assessment of a silver nanoparticle in soil applied via sewage sludge. *Environ. Sci. Eur.* 25, 1–14. <https://doi.org/10.1186/2190-4715-25-17>
6. Blaser et al. (2008) Estimation of cumulative aquatic exposure and risk due to silver: Contribution of nano-functionalized plastics and textiles. *Sci. Total Environ.* 390, 396–409. <https://doi.org/10.1016/j.scitotenv.2007.10.010>

Western Nanofabrication Facility

Western University
Physics and Astronomy Building Room 14
London, Ontario N6A 3K7

nanofab.uwo.ca

Prof. François Lagugné-Labarthet
Facility Director
flagugne@uwo.ca

Todd Simpson Ph.D.
Senior Research Scientist
tsimpson@uwo.ca

Tim Goldhawk
Laboratory Supervisor
tim.goldhawk@uwo.ca

WNF
WESTERN
NANOFABRICATION
FACILITY